RSC Advances




ROYAL SOCIETY OF CHEMISTRY

www.rsc.org/advances

# Graphical abstract

Graphene/polyaniline composites prepared by one-step electrosynthesis of graphene oxide and aniline monomer give a dimensionless thermoelectric figure-of-merit (*ZT*) of 0.009.

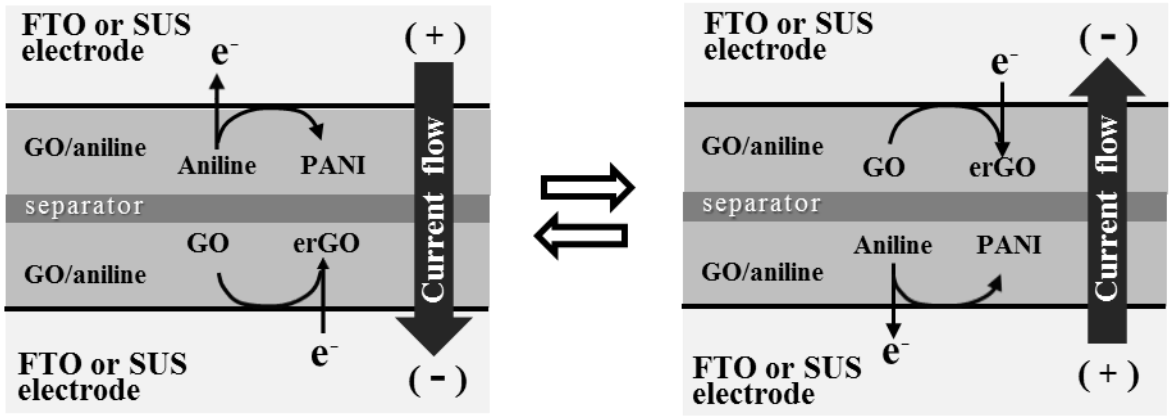

RSC Advances

ARTICLE

# Thermoelectric performances of graphene/polyaniline composites prepared by one-step electrosynthesis

Yutaka Harima,*[a] Saki Fukumoto,[a] Lu Zhang,[a] Xiaoqing Jiang,[b] Jun Yano,[c] Kei Inumaru[a] and Ichiro Imae[a]

Received 00th January 20xx,
Accepted 00th January 20xx

DOI: 10.1039/x0xx00000x

www.rsc.org/

Composite films comprising graphene and polyaniline were prepared in one step by a facile electrochemical technique with graphene oxide (GO) and aniline monomer as raw materials, and their thermoelectric properties were investigated. Electrical conductivities of the composite films generated on the fluorine-doped tin oxide (FTO) electrode were dependent on the weight ratio of GO and aniline, and they exhibited a peak value of 30 S $cm^{-1}$ at the GO/aniline ratio between 5:1 and 10:1, while Seebeck coefficients were less dependent on the weight ratio. The maximum power factor (*PF*) for the composite films was *ca.* 1 μW $m^{-1}$ $K^{-2}$. When the FTO electrode was replaced by the stainless steel electrode, conductivities of the composite films with the GO/aniline ratio of 8:1 were increased up to *ca.* 130 S $cm^{-1}$. As a result, the *PF* and the dimensionless thermoelectric figure-of-merit (*ZT*) at room temperature reached 3.6 μW $m^{-1}$ $K^{-2}$ and 0.008, respectively. The *ZT* value is the highest among those reported so far for graphene/PANI composites. Possible reasons for the conductivity enhancement on the stainless steel electrode are also discussed on the basis of electrochemical measurements and X-ray photoelectron spectroscopy.

## 1. Introduction

Thermoelectric (TE) materials have received much interest because they are capable of directly converting exhaust heat to electricity with no use of moving mechanisms responsible for noises and outages. Their performances are evaluated by a thermoelectric power factor (*PF*) and a dimensionless thermoelectric figure-of-merit (*ZT*) defined by $PF = S^2\sigma$ and $ZT = S^2\sigma T/\kappa$, where $S$, $\sigma$, $\kappa$, and $T$ are Seebeck coefficient, electric conductivity, thermal conductivity, and absolute temperature, respectively. $Bi_2Te_3$, which has been used in a Peltier element, is a typical inorganic TE material giving a *ZT* value close to unity,[1] which is believed to be a numerical target for a practical use of the TE materials. TE materials based on inorganic compounds have been intensively studied so far and those having *ZT* values greater than unity have already been developed.[1] However, the high TE performances of them tend to be realized only at increased temperatures beyond 400 °C, although a large part of exhaust heat from households as well as chemical plants, so-called low-temperature exhaust heat, is known to be below 200 °C and thus TE materials efficient at low temperatures are needed for practical applications. In addition, most of efficient inorganic TE materials developed so far are composed of Bi, Sb, Te, Pb, Co, or Ge, that are expensive, brittle, unstable in air, and even toxic. Very recently, an increasing number of studies have been devoted to organic alternatives to inorganic TE materials. In general, organic compounds are weak against heat compared with inorganic ones, but they can be used for an effective recovery of a low-temperature exhaust heat occupying 70% of a total exhaust heat. Instead, organic TE materials are attractive candidates because of low cost of fabrication due to a plenty of resources and ease of synthesis, light weight, flexibility, and low thermal conductivities leading to high *ZT* values. Conducting polymers match the above conditions and polyaniline (PANI), one of conducting polymers, was an organic TE material studied first by Toshima group in 1999.[2,3] Conducting polymers such as polypyrrole,[4,5] polyphenylenevinylenes,[6] polythiophene,[7] and its derivatives including poly(3,4-ethylene-dioxythiophene):poly(styrenesulfonate) (PEDOT:PSS) have also been investigated as a class of possible organic TE materials. It has been reported that the commercially available PEDOT:PSS films after treatment with organic solvents and/or chemical or electrochemical control of their oxidation levels give the *ZT* values of 0.25,[8] 0.31,[9] and 0.42.[10] Another strategy to improve the TE performances is to fabricate composites by expecting a possible synergistic effect arising from a combination of materials with different properties. Indeed, composites of carbon nanotube (CNT) and conducting polymers were examined and a synergistic effect was found.[11-14] Composites consisting of PANI and graphene oxide (GO) or reduced GO have also been intensively studied.[15-22]

In the present study, graphene/PANI composites prepared by a simple electrochemical technique developed earlier for producing electrochemical capacitors are investigated from the viewpoint of their application to TE materials.[23] The composites with different weight ratios of graphene and PANI are prepared, and their conductivities and Seebeck coefficients are measured at room temperature to evaluate TE performances. It is found that the conductivities of the composite films are

[a] Department of Applied Chemistry, Graduate School of Engineering, Hiroshima University 1-4-1 Kagamiyama, Higashi-Hiroshima, Hiroshima 739-8527, Japan. E-mail: harima@mls.ias.hiroshima-u.ac.jp; Fax: +81-82-424-5494; Tel: +81-82- 424-6534
[b] Jiangsu Key Laboratory of New Power Batteries, Laboratory of Electrochemistry, College of Chemistry and Materials Science, Nanjing Normal University, 122 Ninghai Road, Nanjing 210097, P R China
[c] Department of Engineering Science, Niihama National College of Technology, Yagumocho 7-1, Niihama, Ehime 792-8580, Japan

enhanced by four times when the fluorine-doped tin oxide (FTO) electrode is replaced by the stainless steel (SUS) electrode. The composite films prepared on the SUS electrodes with the GO/aniline weight ratio of 8:1 give the maximum *PF* of 3.6 μW $m^{-1}$ $K^{-2}$ and *ZT* value of 0.008 at room temperature. The conductivity enhancement on the SUS electrode is also discussed on the basis of electrochemical measurements and X-ray photoelectron spectroscopy.

## 2. Experimental

GO was synthesized from a natural graphite powder (SNO-10 from SEC Carbon Ltd.) by a modified Hummers method as described.[24] A desired concentration of GO-dispersed solution was prepared by adding a given amount of GO powder into 10 mL of deionized water and ultrasonicated for one hour to enhance exfoliation. Mixtures of GO/aniline at different weight ratios ($W_{GO}/W_{ANI}$) were prepared by adding a controlled volume of purified aniline into 10 ml of 3 mg $mL^{-1}$ GO dispersion. The GO/aniline mixtures were well dispersed after being sonicated for 10 min. GO/aniline films (0.50 mg) with different GO/aniline weight ratios were prepared by casting a given volume of the above mixtures on an FTO electrode or a thin stainless steel (SUS 304) sheet fixed by a double-face adhesive tape on a glass plate. Surface areas of the GO/aniline films were controlled to be 0.785 $cm^2$ (diameter of the film: 1.0 cm) irrespective of the weight ratio. A photo of the composite film prepared as described below is shown in Fig. 1B.

The structure of the two-electrode cell is shown in Fig. 1A, where a filter paper soaked with acid (2 M $H_2SO_4$) is sandwiched between the two conductive substrates (FTO or SUS) on which GO/aniline films having the same GO/aniline ratios are deposited. The successive triangular-wave voltage between -1.4 and +1.4 V at a scan rate of 100 mV $s^{-1}$ was applied to the electrodes to convert GO to its reduced form (electrochemically reduced GO: erGO) and, concurrently, to oxidize aniline to PANI in the GO/aniline films deposited on the electrodes. Alternatively, the redox cycles were performed by stepping the applied voltage between +1.4 and -1.4 V with a rest time of 20 s at each stepped voltage. As is schematically shown in Fig. 2, the top GO/aniline film will be oxidized to give PANI and the bottom film will be reduced to give erGO. When the voltage is reversed, on the other hand, GO in the top film will be reduced and aniline in the bottom film will be oxidized. Thus, by cycling the voltage between +1.4 and -1.4 V in the voltage-sweep and –step methods, aniline and GO in both films can be simultaneously oxidized and reduced to PANI and erGO, respectively. The voltage of 1.4 V was decided according to our previous work.[23] After the experiment, the two-electrode cell was short-circuited and decomposed to pick up erGO/PANI composite films, and then the free-standing composite films (*ca.* 5 μm in thickness) were subjected to the measurements of conductivity, Seebeck coefficient, and other properties. Conductivities of the composite films were determined by the four-probe method using a resistivity meter (Loresta-GP MCP-T610, Mitsubishi Chemical Corp.). Seebeck coefficients were measured using a custom made set-up composed of thermocouples and Peltier devices. This set-up was calibrated with the Seebeck coefficients of -18 and +22 μV $K^{-1}$ reported for alumel and chromel alloys at room temperature, respectively. XPS spectra of the composite films were taken on an X-ray photoelectron spectroscopy (XPS: ESCA-3400, Kratos Analytical). Film morphologies were observed with a field-emission scanning electron microscope (SEM, JEOL JSM-6320F). Electrochemical measurements were made with an automatic polarization system (Hokuto Denko HSV-100).

## 3. Results and discussion

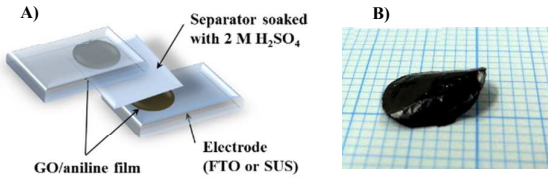


**Fig. 1** A) Illustration of a two-electrode cell for electrochemical conversion of GO/aniline film to erGO/PANI composite and B) photo of erGO/PANI film.

In our previous study,[23] GO/aniline films in the two-electrode cell were converted successfully to erGO/PANI composite films by cycling the voltage between -1.4 and +1.4 V at ±100 mV $s^{-1}$. The

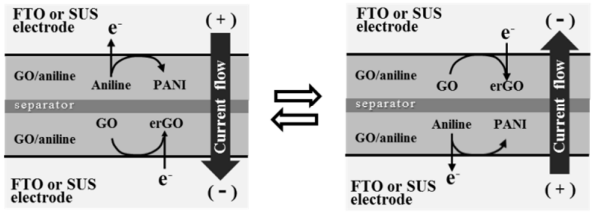


**Fig. 2** Illustration for mechanisms of electrochemical conversion of GO/aniline film to erGO/PANI composite in two-electrode cell.

integral area of the current *vs.* voltage curve during the voltage cycling could be a measure of the extent of the reaction and also provided an integral capacitance of the composite film. In the present study, GO/aniline films was treated in a similar fashion and the voltage cycling was stopped at a given time to decompose the two-electrode cell and pick up thus treated films for the conductivity measurements. Black circles in Fig. 3 depict conductivities of the films obtained in this way, where the $W_{GO}/W_{ANI}$ of GO/aniline film was 8:1 and the FTO electrode was used. The films were almost insulating when the time of the voltage cycling was shorter than 10 hours, whereas the conductivity increased slowly with time and was 20 S $cm^{-1}$ even 15 hours after the start of voltage cycling. In order to shorten the time required for the conversion of GO/aniline to erGO/PANI, a square-wave voltage between +1.4 and -1.4 V was applied to the cell (20 s at each voltage). The conductivities of the composite films converted by the square-wave voltage are shown by blue circles in Fig. 3. As expected, the conductivities increase in much shorter time and level off at ca. 30 S $cm^{-1}$ at 13 hours or later, although the conductivity values of the composite films prepared under the same condition are somewhat scattered. We have already noted that the almost complete conversion to the composite requires longer times when the $W_{GO}/W_{ANI}$ values of the GO/aniline films are larger.[23] In view of this, in the subsequent study, we electrolyzed the GO/aniline in the two-electrode cell for 20 hours irrespective of their

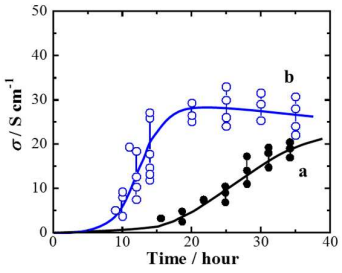


**Fig. 3** Changes in conductivity ($\sigma$) of GO/aniline ($W_{GO}/W_{ANI}$=8) film with electrolysis time, prepared on FTO electrodes by a) voltage-sweep and b) voltage-step methods. In the former method, voltage of the two electrodes was cycled between -1.4 and +1.4 V at a sweep rate of 100 mV $s^{-1}$, while in the latter, voltage was stepped repeatedly between +1.4 and -1.4 V, and kept at respective voltages for 20 s. Weights of the respective GO/aniline films were ca. 0.50 mg. All the curves and the vertical segments in Figs. 3-5 are drawn for guides of eyes.

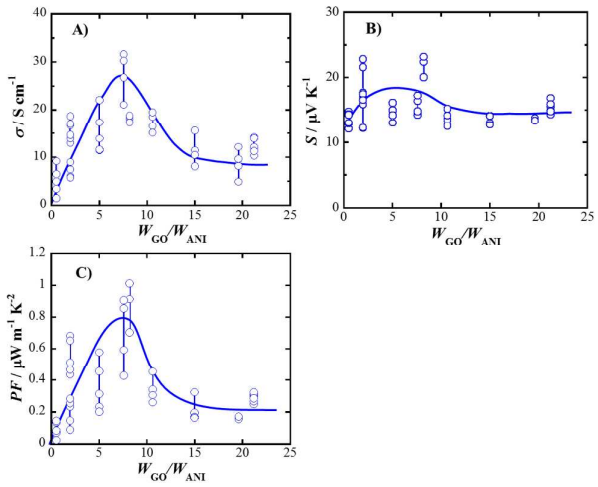


**Fig. 4** Changes in A) conductivity ($\sigma$), B) Seebeck coefficient ($S$), and C) power factor ($PF$) of erGO/PANI composite with GO/aniline weight ratio, $W_{GO}/W_{ANI}$, where GO/aniline films were treated by voltage-step method with FTO electrodes.

composition ($W_{GO}/W_{ANI}$).

Fig. 4 illustrates conductivities ($\sigma$), Seebeck coefficients ($S$), and power factors ($PF$s) of the erGO/PANI films obtained by electrosynthesis of GO/aniline films with different $W_{GO}/W_{ANI}$ values on the FTO electrodes for 20 hours by using the square-wave voltage. It is seen from Fig. 4A that the conductivities increase with the increase of $W_{GO}/W_{ANI}$ and show a broad peak in the range of $W_{GO}/W_{ANI}$ between 5 and 10. By increasing the ratio of GO in the GO/aniline film further, the conductivities dropped to around 10 S cm$^{-1}$. Fig. 4B depicts a plot of Seebeck coefficient against $W_{GO}/W_{ANI}$. The Seebeck coefficients are positive, demonstrating that main charge carriers in the composites have a positive sign. As is the case of conductivities, Seebeck coefficients of the composite films are scattered, but we see that they are not dependent much on $W_{GO}/W_{ANI}$ compared with the conductivities. Fig. 4C depicts power factors of the composite films calculated with the data shown in Figs. 4A and 4B. The figure shows clearly that there is a $W_{GO}/W_{ANI}$ value which gives a maximum power factor of *ca.* 1 μW m$^{-1}$ K$^{-2}$. By referring to this result, the GO/aniline films of $W_{GO}/W_{ANI}$ = 8 were employed for examining an influence of an electrode material as described below.

In Fig. 5 are compared the TE properties of the GO/aniline films ($W_{GO}/W_{ANI}$ = 8) treated with the FTO and SUS electrodes using the voltage-step technique (±1.4 V). As shown in Fig. 5A, conductivities of the composite films prepared with SUS (red) start to increase with a lapse of electrolysis time without delay like the case of FTO (blue) and reach *ca.* 130 S cm$^{-1}$ 10 hours after the start of electrolysis, being followed by the decrease of conductivities by further electrolysis. It is likely that the conductivity decrease is due to overoxidation of PANI on the SUS electrode. Seebeck coefficients were also measured for the composite films prepared on FTO and SUS electrodes and the results are depicted in Fig. 5B. In contrast to the case of conductivities, the Seebeck coefficients were almost independent of the electrolysis time for both FTO and SUS electrodes, and were around 16 μV K$^{-1}$ irrespective of the difference of the electrode materials, although the Seebeck coefficients for the FTO electrode were small in the short electrolysis time. It is well-

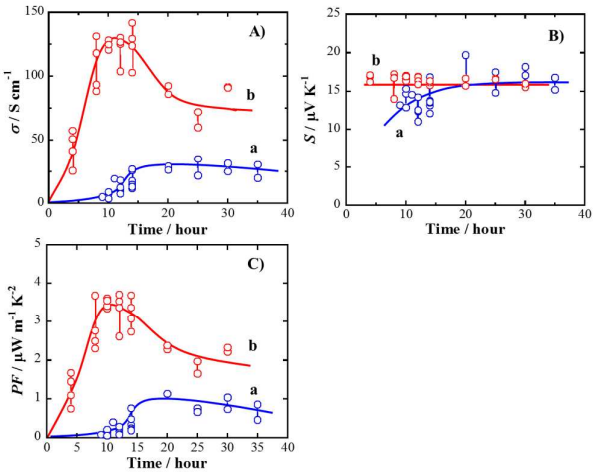


**Fig. 5** Changes in A) conductivity ($\sigma$), B) Seebeck coefficient ($S$), and C) power factor ($PF$) of GO/aniline ($W_{GO}/W_{ANI}$=8) films with electrolysis time, where GO/aniline films were treated by voltage-step method with a) FTO and b) SUS electrodes.

known in TE materials studies that there is a trade-off relation between conductivity ($\sigma$) and Seebeck coefficient ($S$). It is likely that such a relation does not hold for the erGO/PANI composites: a large change in $\sigma$ with a negligible change in $S$ with the electrolysis time. It is known that the Seebeck coefficient ($S$) is explained by the following equation:[25]

$$S = \frac{\pi^2 k_B{}^2 m^* T}{(3\pi^2)^{\frac{2}{3}} \hbar e n^{\frac{2}{3}}} \qquad (1)$$

where $m^*$ denotes the effective mass of charge carriers, $n$ the density of charge carriers, and $k_B$, $\hbar$, $T$, and $e$ have their usual significances. Thus, almost constant values of $S$ in Fig. 5B suggest that the density of charge carriers ($n$) does not change with the electrolysis time so far as the $m^*$ value is constant. On the other hand, the electrical conductivity ($\sigma$) is a product of $n$ and the charge carrier mobility ($\mu$) as expressed by $\sigma = en\mu$. Therefore, the $\sigma$ values should not change when the $n$ and $\mu$ values do not change. Nevertheless, the $\sigma$ values change with the electrolysis time as shown in Fig. 5A. Consequently, the observed change of $\sigma$ is likely to be ascribed to the development of electrically conductive domains in the GO/aniline film with the increase in the electrolysis time.

Fig. 5C depicts the power factors of the composite films prepared with the SUS electrode in comparison with those with the FTO electrode. The maximum power factor for the former films is close to 3.6 μW m$^{-1}$ K$^{-2}$ when the electrolysis time is 10 hours, while the power factor for the latter film is less than 1 μW m$^{-1}$ K$^{-2}$. Very recently, thermal conductivities of reduced graphene oxide-polyaniline composites have been reported to be 0.1078 to 0.1433 W m$^{-1}$ K$^{-1}$ for 0 to 80 wt% of reduced GO, less dependent on the composition ratio.[21] If we assume the thermal conductivity of the erGO/PANI film ($W_{GO}/W_{ANI}$ = 8) as 0.13 W m$^{-1}$ K$^{-1}$, one can evaluate the maximum $ZT$ value for the composite films as 8x10$^{-3}$ at room temperature. This $ZT$ value is much smaller than those for the PEDOT:PSS films,[8-10] but is high compared with those reported so far for graphene/polyaniline composites: 1.37×10$^{-3}$,[15] 1.26 x 10$^{-4}$,[17] 4.86 x10$^{-4}$,[18] 1.95x10$^{-3}$,[20] 4.23x10$^{-4}$,[21] and 4.6x10$^{-3}$.[22] It is also much greater than those for PANI alone.[3]

**Table 1** Fitted results (%) of C1s XPS spectra of erGO/PANI composites prepared on FTO and SUS electrodes

| Electrode | Peak 1<br>C-C ($sp^2$)<br>284.3 eV | Peak 2<br>C-C ($sp^3$ defect)<br>285.15 eV | Peak 3<br>C-O(hydroxyl and epoxy)<br>286.5 eV | Peak 4<br>C=O (carbonyl)<br>287.8 eV | Peak 5<br>O-C=O (carboxyl)<br>289.1 eV |
|---|---|---|---|---|---|
| FTO | 28.3 | 38.5 | 13.7 | 5.3 | 14.2 |
| SUS | 38.9 | 32.2 | 10.1 | 4.7 | 14.1 |

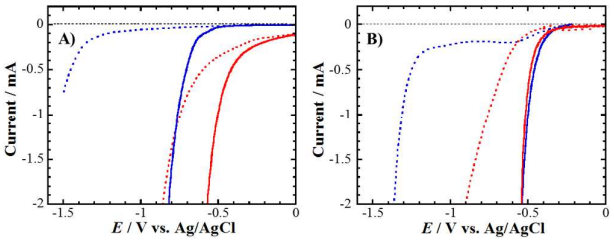


**Fig. 6** Linear-sweep voltammograms (LSVs) of A) FTO and B) SUS electrodes in aqueous solutions of 0.1 M KCl (broken line) and 2 M $H_2SO_4$ (solid line) at 50 mV $s^{-1}$. LSVs on GO-deposited FTO and GO-deposited SUS electrodes are also included in the figure and expressed by red lines, while those on bare FTO and SUS electrodes are by black

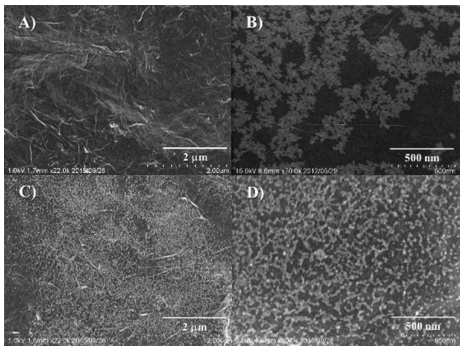


**Fig. 7** SEM images of erGO/PANI composites obtained by electrolysis of GO/aniline ($W_{GO}/W_{ANI}$=8) films on A) and B) FTO, and C) and D) SUS electrodes.

We will now discuss the reason for the conductivities of the erGO/PANI composites enhanced by the use of the SUS electrode. Fig. 6A depicts linear-sweep voltammograms (LSVs) of FTO and GO-deposited FTO electrodes measured with a three-electrode system in aqueous solutions of 0.1 M KCl and 2 M $H_2SO_4$, while Fig. 6B denote LSVs on SUS and GO-deposited SUS electrodes in the same solutions. On the bare FTO electrode in KCl solution (black broken curve), only small cathodic currents flow at potentials more positive than -1.4 V. In the $H_2SO_4$ solution, the cathodic current rise starts at 0.7 V, which is shifted to a positive direction (black solid curve) due to the reduction of protons on the FTO electrode. LSVs of GO-deposited FTO in KCl and $H_2SO_4$ solutions (red broken curve) suggest that the reduction of GO deposited on FTO takes place in KCl solution and the GO reduction is slightly enhanced in $H_2SO_4$. Here, by comparing LSVs of FTO and GO-deposited FTO electrodes in the $H_2SO_4$ solution, we see that in the two-electrode cell, GO on FTO will be reduced without appreciable evolution of hydrogen gas. As is shown in Fig. 6B, on the other hand, protons are more easily reduced on SUS than FTO because of a low hydrogen overpotential of SUS and GO deposited on SUS is reduced at the same potentials as the reduction of protons. Therefore, one can presume that in the two-electrode cell experiments with SUS, the electrochemical reduction of GO may take place concurrently with the evolution of hydrogen gas on the surface of SUS. On this basis, we presume that the relatively high conductivities of the erGO/PANI composites prepared with SUS are due to an efficient conversion of

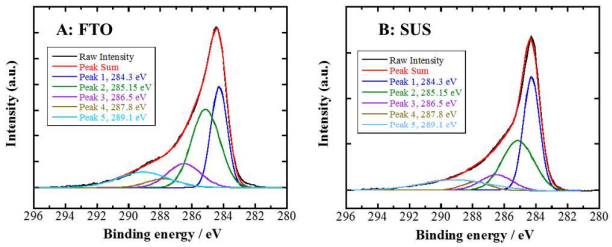


**Fig. 8** XPS spectra for C1s of erGO/PANI ($W_{GO}/W_{ANI}$=8) composite films obtained by voltage-step method with A) FTO and B) SUS electrodes.

GO to erGO by the electrochemical reduction of GO in the presence of a highly reducing hydrogen gas.

The erGO/PANI composites were prepared by using the voltage-step technique (±1.4 V, 10 hours) with the FTO and SUS electrodes and the SEM images of the obtained composite films are shown in Fig. 7. At low magnification, both the surfaces of the composites prepared with FTO and SUS show a wrinkled structure characteristic of GO. A clear difference is seen in the SEM images taken at high magnification: PANI nanoparticles are dispersed better in the erGO/PANI composite prepared with SUS than in those obtained with FTO. The more uniformly-dense distribution of the PANI nanoparticles for the composites obtained with the SUS electrode may be related to the evolution of hydrogen gas during preparation of the composites.

Figs. 8A and 8B show the C1s XPS spectra of the erGO/PANI-8:1 films ($W_{GO}/W_{ANI}$ = 8) prepared with the FTO and SUS electrodes, respectively, and detailed information of each peak in the fitted results of the C1s XPS spectra is summarized in Table 1. The composite film (FTO) contains 33.2% oxygenated carbons including 13.7% C–O (hydroxyl and epoxy) centered at 286.5 eV, 5.3% C=O (carbonyl) at 287.8 eV, and 14.2% O-C=O (carboxyl) at 289.1 eV.[26,27] Carbon atoms of 66.8% are nonoxygenated, including 28.3% $sp^2$ carbons at 284.3 eV and 38.5% $sp^3$ carbons (defect) at 285.15 eV.[26,27] When the SUS electrode is used in the two-electrode cell, on the other hand, $sp^2$ carbons increase from 28.3% to 38.9% with a slight decrease of $sp^3$ carbons (38.5% to 32.2%). The nonoxygenated carbon groups in erGO/PANI (SUS) increase from 66.8% to 71.1%, suggesting that the oxygen-containing functional groups are removed effectively by using SUS in place of FTO. The effective removal of the oxygen species on the SUS electrode can be a reason for the formation of highly conductive erGO/PANI composites.

## 4. Conclusions

Composite films of graphene/polyaniline were prepared by a one-step electrochemical technique with GO and aniline monomer, and their thermoelectric performances were

optimized with respect to the electrolysis time and the weight ratio of GO and aniline. It was found that the electrical conductivities of the composite films can be enhanced *ca.* four times by employing SUS in place of FTO, while no appreciable change was observed for the Seebeck coefficients. The composite films of the GO/aniline weight ratio of 8:1 prepared on the SUS electrodes gave the maximum power factor of 3.6 $\mu W\ m^{-1}\ K^{-2}$ and *ZT* value of 0.008 at room temperature. In addition, the conductivity enhancement on the SUS electrode were accounted for in terms of the efficient removal of oxygen species of GO by the direct electrochemical reduction of GO on SUS concurrently with the reduction of GO by hydrogen gas generated by reduction of protons on SUS.

## Acknowledgements

Y.H. and I.I. wish to thank Yukihisa Hosino of Denka for inspiring us to this research field. They also thank Takao Mori, Yoshikazu Shinohara, Masayuki Takeuchi of National Institute for Materials Science, and Yasunari Sakurai of Denka for their fruitful discussions. Thanks are also due to Yibin Xu for preliminary measurements of thermal diffusivities of the composite films.

## Notes and references

1 A recent progress on inorganic thermoelectric materials is reviewed in K. Kumoto and T. Mori (Eds.), Springer, Dordrecht, 2013.
2 H. Yan and N. Toshima, *Chem. Lett.*, 1999, 1217.
3 N. Toshima, *Macromol. Symp*., 2002, 185, 81.
4 D. S. Maddison and J. Unsworth, *Synth. Metals*, 1988, 26, 99.
5 N. Mateeva, H. Niculescu, J. Schenoff and L.R. Testardi, *J. Appl. Phys.*, 1998, 83, 3111.
6 Y. Hiroshige, M. Ookawa and N. Toshima, *Synth. Metals*, 2006, 156, 1341.
7 K. Hiraishi, A. Masuhara, H. Nakanishi, H. Oikawa and Y. Shinohara, *Jpn. J. Appl. Phys.*, 2009, 48, 071501.
8 O. Bubnova, Z.U. Khan, A. Malti, S. Braun, M. Fahlman, M. Berggren and X. Crispin, *Nature Mater.*, 2011, 10, 429.
9 S.H. Lee, H. Park, S. Kim, W. Son, I.W. Cheong and J.H. Kim, *J. Mater. Chem. A*, 2014, 2, 7288.
10 G-H. Kim, L. Shao, K. Zhang and K.P. Pipe, *Nature Mater.*, 2013, 12, 719.
11 C. Meng, C. Liu and S. Fan, *Adv. Mater.*, 2009, 22, 535.
12 Q. Yao, L. Chen, W. Zhang, S. Liufu and X. Chen, *ACS Nano*, 2010, 4, 2445.
13 D. Kim, Y. Kim, K. Choi, J.C. Grunlan and C. Yu, *ACS Nano*, 2010, 4, 513.
14 C. Yu, K. Choi, Y. Liang and J.C. Grunlan, *ACS Nano*, 2010, 5, 7885.
15 L. Wang, D. Wang, G. Zhu, J. Li and F. Pan, *Mater. Lett.*, 2011, 65, 1086.
16 Y. Du, S. Z. Shen, W. Yang, R. Donelson, K. F. Cai and P. S. Casey, Synth. Metals, 2012, 161, 2688.
17 J. L. Xiang and L. T. Drzal, Polymer, 2012, 53, 4202.
18 Y. Zhao, G. S. Tang, Z. Z. Yu and J. S. Qi, Carbon, 2012, 50, 3064.
19 B. Abad, I. Alda, P. Diaz-Chao, H. Kawakami, A. Almarza, D. Amantia, D. Gutierrez, L. Aubouy and M. Martin-Gonzalez, *J. Mater. Chem. A*, 2013, 1, 10450.
20 Y. Lu, Y. Song and F. P. Wang, *Mater. Chem. Phys.*, 2013, 138, 238.
21 W. Wang, Q. Zhang, J. Li, X. Liu, L. Wang, J. Zhu, W. Luo and W. Jiang, *RSC Adv.*, 2015, 5, 8988.
22 M. Mitra, C. Kulsi, K. Chatterjee, K. Kargupta, S. Ganguly, D. Banerjee and S. Goswami, *RSC Adv.*, 2015, 5, 31039.
23 X. Jiang, S. Setodoi, S. Fukumoto, I. Imae, K. Komaguchi, J. Yano, H. Mizota and Y. Harima, *Carbon*, 2014, 67, 662.
24 Y.X. Xu, H. Bai, G.W. Lu, C. Li and G.Q. Shi, *J. Amer. Chem. Soc.*, 2008, 130, 5856.
25 Y. Chen, Y. Zhao and Z. Liang, *Energy Environ. Sci.*, 2015, 8, 401.
26 Y.Y. Shao, J. Wang, M. Engelhard, C. Wang and Y. Lin, *J Mater. Chem.*, 2010, 20, 743.
27 X.Y. Peng, X.X. Liu, D. Diamond, K.T. Lau, Carbon 49 (2011) 3488.